Natural and anthropogenic modes of surface temperature variations in the last thousand years

E. Zorita,[1] J. F. González-Rouco,[2] H. von Storch,[1] J. P. Montávez,[3] and F. Valero[2]

Received 14 September 2004; revised 10 March 2005; accepted 22 March 2005; published 27 April 2005.

[1] The spatial patterns of surface air-temperature variations in the period 1000 to 2100, simulated with the ECHO-G atmosphere-ocean coupled model, are analyzed. The model was driven by solar, volcanic and greenhouse gas forcing. The leading mode of temperature variability in the preindustrial period represents an almost global coherent variation of temperatures, with larger amplitudes over the continents and Northern Hemisphere. This mode also describes a large part of the spatial structure of the warming simulated in the 21st century. However, in the 21st century, regional departures from this spatial structure are also present and can be ascribed to atmospheric circulation responses to anthropogenic forcing in the last decades of the 21st century. **Citation:** Zorita, E., J. F. González-Rouco, H. von Storch, J. P. Montávez, and F. Valero (2005), Natural and anthropogenic modes of surface temperature variations in the last thousand years, *Geophys. Res. Lett.*, *32*, L08707, doi:10.1029/2004GL021563.

1. Introduction

[2] The assessment of the recently observed climate warming and its potential anthropogenic origin has prompted the need to understand and estimate climate changes through the last millennium. Efforts have relied both on the statistical reconstruction using proxy data [*Briffa and Osborn*, 2002; *Jones and Mann*, 2004] and model simulations of past climate states.

[3] The modeling approach has made use of models of varying complexity and experiment design, mostly focused on the impacts of solar variability on climate [*Haigh*, 1999]. However, results with paleo simulations of the last millennium support the idea that the global warming of the last decades cannot be explained only by changes in natural variability and solar forcing [*Crowley*, 2000; *Bauer et al.*, 2003; *Cubasch et al.*, 1997].

[4] Since natural and anthropogenic forcings have been important in last millennium climate variations, the question arises whether their spatial signatures are similar. Simulations with three-dimensional climate models are scarce due to computational limitations and, although burdened with an unsatisfactory level of uncertainties (e. g., exact forcings, climate sensitivity...), they constitute a powerful tool to address such questions. *Cubasch et al.* [1997] presented integrations with a coupled atmosphere-ocean GCM forced with solar variability estimations since 1700 A.D. The surface temperature response pattern was dominated by the land-sea contrast and broadly resembled the pattern obtained in greenhouse-gas simulations [*Intergovernmental Panel on Climate Change* (*IPCC*), 2001]. More recently, several simulations of the last 500 years with a climate model with a more realistic representation of the stratosphere and its photochemistry, lead to the conclusion that the spatial surface warming patterns associated with solar and anthropogenic greenhouse forcing are virtually indistinguishable in an assessment of differences between present time and the Late Maunder Minimum [*Rind et al.*, 2004]. This may support the idea that the response of near-surface temperature to external forcing, independently of its nature, may strongly project to the same patterns of variability [*Corti et al.*, 1999]. This is supported by studies of anthropogenic climate change scenarios [*Fyfe et al.*, 1999] and time slice paleoclimate simulations [*Shindell et al.*, 2001] which show sensitivity of circulation regimes to changes in external forcing.

[5] This work explores the surface temperature response of a 'state-of-the-art' atmosphere-ocean GCM to changes in natural and anthropogenic external forcing through a climate simulation of the last 1000 years, continued to the end of the 21st century under the IPCC SRES A2 scenario, which provides a frame for comparison of stronger radiative forcing. We address the question of whether there is a unique pattern of temperature response which characterizes the industrial versus the preindustrial era and of which dynamical mechanisms of the atmosphere are excited with industrialization. Results indicate that the temperature response to anthropogenic forcing projects on a pattern of forced variability which existed in preindustrial times. However, when greenhouse gases loading becomes particularly strong, it can excite atmospheric circulation trends which are related to regional deviations from the leading preindustrial temperature variability pattern.

2. Model and Experiment Design

[6] The integrations analyzed herein were produced with the ECHO-G atmosphere-ocean GCM. This model consists of the spectral atmospheric model ECHAM4 and the ocean model HOPE-G [*Legutke and Voss*, 1999] and constitutes a more recent version than that used by *Cubasch et al.* [1997]. The model ECHAM4 is used with a horizontal resolution T30 ($\sim 3.75^\circ \times 3.75^\circ$). The horizontal resolution of the ocean model component is approximately $2.8^\circ \times 2.8^\circ$, with a grid refinement in the tropical regions. A flux adjustment constant in time was applied to avoid climate drift.

[7] The model was forced with estimations of external forcing factors for the period 1000 to 1990 A.D. (Figure 1a):

[1]Institute for Coastal Research, GKSS-Research Centre, Geesthacht, Germany.
[2]Departamento de Astrofísica y CC. de la Atmósfera, Universidad Complutense de Madrid, Madrid, Spain.
[3]Departamento de Física, Universidad de Murcia, Murcia, Spain.

0094-8276/05/2004GL021563$05.00

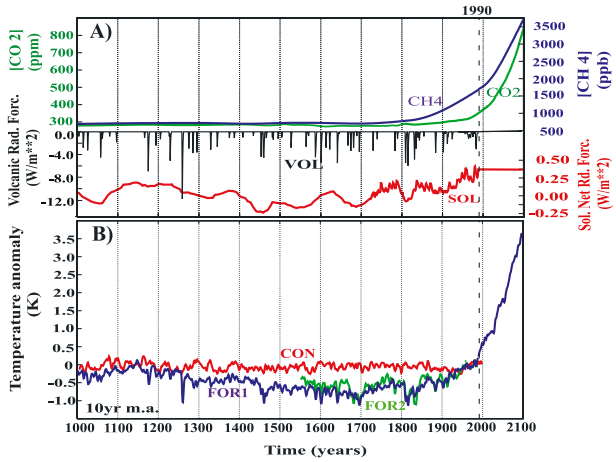

Figure 1. (a) Estimations of greenhouse gases (CO_2,CH_4), solar irradiance (SOL) and changes in atmospheric reflectivity in the stratosphere (VOL) used to force the model. (b) Forced integrations (FOR1,FOR2) and control (CON) global temperature anomalies (reference period was the last 30 years in CON and 1961–90 in FOR1,2).

solar variability (*SOL*), atmospheric greenhouse gas concentrations (CO_2 and CH_4), and radiative effects of stratospheric volcanic aerosols (*VOL*), derived from the reconstructions provided by *Crowley* [2000]. For the 1990 to 2100 A.D. interval *SOL* and *VOL* where kept constant and greenhouse gases were varied according to SRES scenario A2 [*IPCC*, 2001]. Hereafter industrial times (anthropogenic influence) will refer to the period after 1800 A.D., when the increase in greenhouse gases is noticeable. Next to changes in atmospheric composition, Figure 1a also depicts the higher solar irradiance in the Medieval Optimum (MO, ca. 10th to 13th century) and the lower values in the Little Ice Age (LIA, ca. 14th to 19th century), as well as shorter anomalous periods within the LIA like the Spoerer Minimum (SM, ca. 1450 A.D.), the Late Maunder Minimum (LMM, ca. 1700 A.D.) and the Dalton Minimum (DM, ca. 1800 A.D.).

[8] The study analyzes two forced integrations covering the period 1000 to 2100 A.D. (FOR1) and 1550 to 1990 A.D. (FOR2) by means of an empirical orthogonal function (EOF) analysis. Further description and results with these simulations are specified by *Zorita and González-Rouco* [2002], and *González-Rouco et al.* [2003]. It should be noted that the simulations studied herein do not take into account the potential effects of sulphate aerosol changes. These could produce a somewhat different regional response to that described herein. The obtained results should be considered within the limits of the forcing factors described in Figure 1a.

3. Results

[9] Figure 1b shows annual global temperature anomalies in FOR1,2 (reference period 1961–1990). Values of a 1000 yr long control (CON) simulation [*Zorita et al.*, 2003] with constant external forcing are also shown for comparison (reference period last 30 years). The model simulates relatively warm temperatures during the 11th and 12th centuries of comparable magnitude to those in the early to mid 20th century. After the 13th century temperatures decline until the early 19th century when the cooling trend is reversed by the increase of solar irradiance and the emissions of greenhouse gases during the industrial period. During the preindustrial cooling trend, anomalous periods arise which match in timing with the SM, LMM and the DM (SOL, Figure 1a). The simulation under the A2 scenario produces a further global warming of about 3.5 K at the end of the 21st century (middle range of the *IPCC* [2001] estimates).

[10] Figure 1 shows there is a good correspondence of the temperature response of the model to solar forcing: about 40% of variance is shared between solar irradiance and temperature. Also worth a comment is the similarity of the simulation to the proxy reconstructions. The correlation of 5-yr low pass filtered global temperatures in FOR1(FOR2) with the reconstruction of *Jones et al.* [1998] is 0.76 (0.75); for the NH simulated averages and *Mann et al.* [1999] reconstruction correlations are 0.63 (0.61) (all values calculated over the periods of overlap). The amplitude of the LIA cooling is however larger in the simulation than in the reconstructions as in some other GCM simulations [*Jones and Mann*, 2004]. Although ideally reconstructions and simulations should present similar evolutions this goal is still difficult to achieve due to uncertainties in reconstructions, forcing estimation and model sensitivity. However, the climate model should be able to produce an internally consistent climate which in many aspects resembles the observed climate.

[11] Figure 2 allows for a joint spatial and temporal description of the temperature changes through FOR1. Figure 2a compares the first principal component (PC)

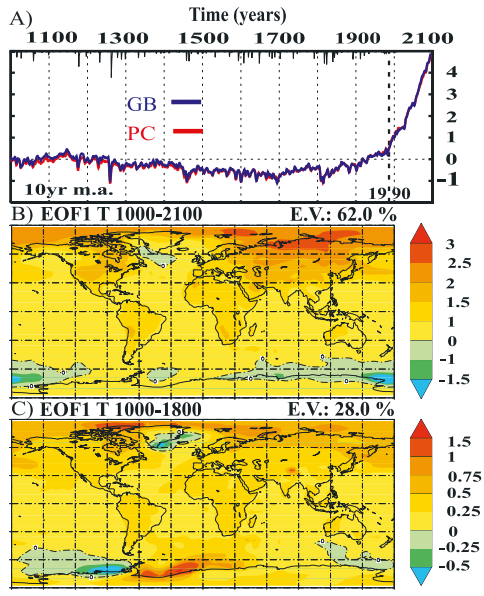

Figure 2. (a) Standardized global temperature averages (GB) in FOR1 and first principal component (PC) resulting from an EOF analysis of the 1000–2100 period in the simulation. The black line shows for comparison the volcanic events (VOL in Figure 1a). (b) Eigenvector corresponding to the principal component in (a). (c) First eigenvector of EOF analysis for the period 1000–1800. Eigenvectors indicate typical variable units.

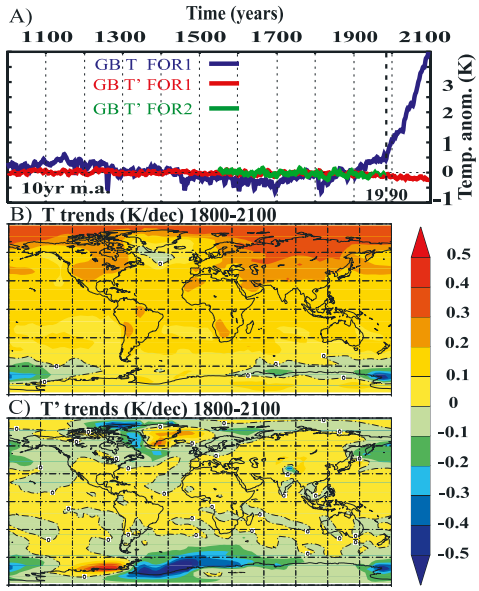

Figure 3. (a) Global averages of temperature anomalies (T) in FOR1 and residuals (T') in FOR1,2. (b) Spatial distribution of temperature trends (K/dec) in FOR1, 1800–2100. (c) As (b) but for residuals.

resulting of an EOF Analysis of annual global surface temperature for the period 1000–2100 with the evolution of global temperatures (GB). Both series are closely related (correlation 0.99). This first mode accounts for 62.0% of the variance and describes the SM, LMM, DM and the last centuries warming. It also highlights cooling events synchronized with volcanic eruptions. The first eigenvector associated to this mode is shown in Figure 2b. In the global scale the pattern describes consistently positive values over which land-sea contrasts arise, with the largest weights occurring mostly over the continents and the high latitudes of both hemispheres. The result agrees with the land-sea contrast pattern suggested by *Cubasch et al.* [1997] for a solar forced integration and also for those of future greenhouse scenarios [*IPCC*, 2001]. According to Figures 2a and 2b there is a single mode of temperature response which is able to represent the major natural and anthropogenic aspects of the simulated global climate variations for the period 1000 to 2100. Comparable results are obtained for FOR2 (not shown). This pattern is not present in the control simulation [*Zorita et al.*, 2003], thus it stems from the imposed external forcing.

[12] A priori, one could expect a somewhat different response for the temperature history before and after industrialization. The first eigenvector of temperature for the preindustrial period is shown in Figure 2c. In spite of some regional scale differences and the obvious change in the magnitude of the loadings, the global scale structure is still comparable in both patterns (spatial correlation 0.61): positive loadings are found almost everywhere with higher values over the continents and northern part of the Northern Hemisphere (NH) and negative values in southeastern Greenland and around Antarctica.

[13] The global similarity in both patterns poses the question of whether the pre-1800 eigenvector (Figure 2c) can account for changes in global temperature during both pre- and post- industrial times. This would suggest that the last two centuries of warming project on a pattern of variability which existed before 1800 A.D., when the concentrations of greenhouse gases can be regarded as constant.

[14] In order to test this hypothesis the signal of the pre-1800 eigenvector was filtered out from the simulated surface temperature and the remaining residuals for the period 1800 to 2100 analyzed. Denoting as $T(x, t)$ the annual temperature anomalies of the period 1000 to 2100 with respect to the average of the interval 1000 to 1800, the influence of the pre-1800 EOF ($e_{pre}(x)$, Figure 2c) can be subtracted from $T(x, t)$ through:

$$T'(x,t) = T(x,t) - e_{pre}(x)\ \alpha(t)$$

where $T'(x, t)$ are the residuals and $\alpha(t)$ the coefficient scores of $e_{pre}(x)$ for the 1000 to 2100 period [*von Storch and Zwiers*, 1999] ($\langle\ \rangle$ denotes inner product):

$$\alpha(t) = \langle e_{pre}(x), T(x,t)\rangle$$

[15] Figure 3a presents global anomalies of temperature (T) and residuals (T') relative to the 1000–1800 period in FOR1. For comparison, the corresponding values for FOR2 are also shown. The peaks associated with the volcano eruptions have vanished and the cooling during the SM, LMM and DM has been reduced to the level of background variability. Further, though a slight cooling trend remains after filtering (see bellow), the residuals do not present any sign of the global warming trend through 1800–2100. This result shows that the preindustrial eigenvector accounts well for the global warming in the industrial era as well as for the changes in solar irradiance and the short term effect of volcanic loads. Figures 3b and 3c show the spatial distribution of decadal trends in T and T' for the period 1800–2100. The original distribution of warming trends in Figure 3b resembles the global scale structure of the eigenvector in Figure 2c. This pattern is filtered in the above process and leads to a trend distribution in the residuals with a prominent regional character (Figure 3c). When spatially averaged, the positive and negative trends in NH cancel out, whereas the SH contributes with a negative trend of 0.01 K/dec since 1990 depicted in Figure 3a.

[16] Regional trends in Figure 3c could be potentially related to changes in large scale circulation modes. This was assessed by splitting the residuals in FOR1 into three broad regions: NH extratropics, tropical regions and the Southern Hemisphere (SH) extratropics. Figure 4 shows the first EOF modes of the temperature residuals (shading) and of sea level pressure (SLP, overlaid contours) in those regions. For the NH and the SH extratropics the annular modes (Arctic and Antarctic Oscillations) arise as the main patterns of SLP variability. For the tropical areas the ENSO variability arises. The principal components corresponding to the residual temperature and the SLP are related in all cases (correlation 0.87, 0.60 and 0.76 for the NH, the tropics and the SH, respectively). Thus Figure 3 shows that regional temperature variability and trends in $T'(x, t)$ are related to the dynamical modes of circulation.

4. Conclusions

[17] Simulations of the last millennium with the ECHO-G model driven with the estimations of past external radiative

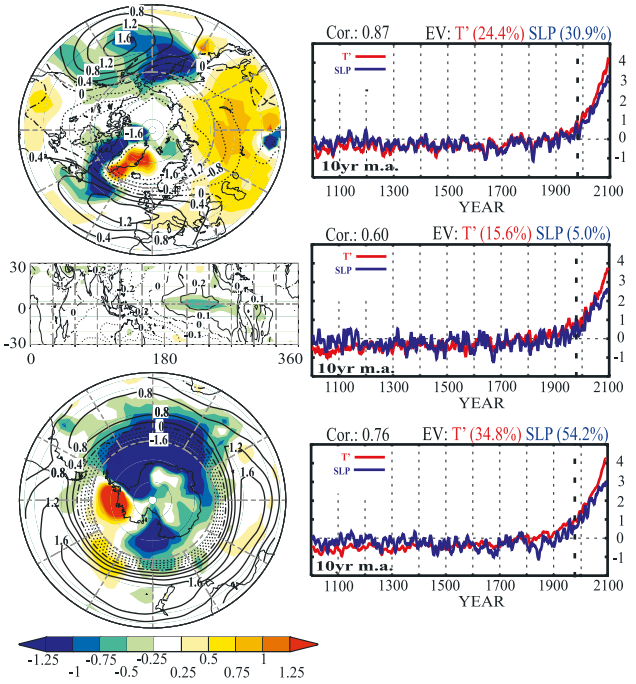

Figure 4. First eigenvector ([T']: K; [SLP]: hPa) and associated principal component (standardized) of residual surface temperature (T', shading) and SLP (contours) in the three latitude bands for the period 1000 to 2100. Exception: for the middle panel, the 4th SLP mode is shown since it correlated best with the first PC of surface temperature.

forcings (solar, volcanic and greenhouse gases) reveal a temperature response which is qualitatively similar to reconstructions and strongly resembles the solar irradiance evolution punctuated by volcanic events.

[18] The spatial and temporal characteristics of the temperature response are well described by the first EOF mode of global surface temperature both for the preindustrial variability and the main warming structure after 1800 A.D. The leading eigenvector broadly resembles patterns of temperature change obtained both in paleoclimate simulations forced with solar irradiance and those of future greenhouse scenarios.

[19] The deviations in the first eigenvector of surface temperature after the beginning of industrialization do not lead in this simulation to a distinct anthropogenic warming pattern. These deviations seem to be ascribed to arising trends of major circulation patterns such as the AO, ENSO and the AAO. Detailed behaviour of temperature changes at regional scales requires a further thorough assessment involving also other circulation modes which can potentially turn out to be model dependent [*Zorita and González-Rouco*, 2000]. These results suggest that the climate response to external forcing can be described in terms of a global response pattern related to land-sea contrasts and regional responses which are related to changes in circulation regimes.

[20] **Acknowledgments.** We thank the two reviewers and Drs. D. Bray, J. Luterbacher, M. Montoya and E. Xoplaki for their comments and proof reading of this manuscript. This work was partially funded by the DEKLIM Program of the German BMBF, the EU project SO&P and by the project REN-2000-0786Cli of the Spanish CICYT.

References

Bauer, E., M. Claussen, V. Brovkin, and A. Huenerbein (2003), Assessing climate forcings of the Earth system for the past millennium, *Geophys. Res. Lett.*, *30*(6), 1276, doi:10.1029/2002GL016639.

Briffa, K. R., and T. J. Osborn (2002), Blowing hot and cold, *Science*, *295*, 2227–2228.

Corti, S., F. Molteni, and T. N. Palmer (1999), Signature of recent climate change in frequencies of natural atmospheric circulation regimes, *Nature*, *398*, 799–802.

Crowley, T. J. (2000), Causes of climate change over the past 1000 years, *Science*, *289*, 270–277.

Cubasch, U., R. Voss, G. C. Hegerl, J. Waszkewitz, and T. J. Crowley (1997), Simulation of the influence of solar radiation variations on the global climate with an ocean-atmosphere general circulation model, *Clim. Dyn.*, *13*, 757–767.

Fyfe, J. C., G. J. Boer, and G. M. Flato (1999), The Arctic and Antarctic Oscillations and their projected changes under global warming, *Geophys. Res. Lett.*, *26*, 1601–1604.

González-Rouco, F., H. von Storch, and E. Zorita (2003), Deep soil temperature as proxy for surface air-temperature in a coupled model simulation of the last thousand years, *Geophys. Res. Lett.*, *30*(21), 2116, doi:10.1029/2003GL018264.

Haigh, J. D. (1999), Modelling the impact of solar variability on climate, *J. Atmos. Sol. Terr. Phys.*, *61*, 63–72.

Intergovernmental Panel on Climate Change (IPCC) (2001), *Climate Change 2001: The Scientific Basis: Contribution of Working Group I to the Third Assessment Report of the Intergovernmental Panel on Climate Change*, edited by J. T. Houghton et al., 881 pp., Cambridge Univ. Press, New York.

Jones, P. D., and M. E. Mann (2004), Climate over past millennia, *Rev. Geophys.*, *42*, RG2002, doi:10.1029/2003RG000143.

Jones, P. D., K. R. Briffa, T. P. Barnett, and S. F. B. Tett (1998), High-resolution paleoclimatic records for the last millenium: Interpretation, integration and comparison with general circulation model control-run temperatures, *Holocene*, *8*, 455–471.

Legutke, S., and R. Voss (1999), The Hamburg atmosphere-ocean coupled circulation model ECHO-G, *DKRZ Tech. Rep. 18*, Dtsch. Klimarechenzentrum, Hamburg, Germany.

Mann, M. E., R. S. Bradley, and M. K. Hughes (1999), Northern Hemisphere temperatures during the past millenium: Inferences, uncertainties and limitations, *Geophys. Res. Lett.*, *26*, 759–762.

Rind, D., D. Shindell, J. Perlwitz, and J. Lerner (2004), The relative importance of solar and anthropogenic forcing of climate change between the Maunder Minimum and the present, *J. Clim.*, *17*, 906–929.

Shindell, D. T., G. A. Schmidt, M. E. Mann, D. Rind, and A. Waple (2001), Solar forcing of regional climate change during the Maunder Minimum, *Science*, *294*, 2149–2152.

von Storch, H., and F. Zwiers (1999), *Statistical Analysis in Climate Research*, Cambridge Univ. Press, New York.

Zorita, E., and J. F. González-Rouco (2000), Desagreement in North Atlantic Oscillation predictions and implications for global warming, *Geophys. Res. Lett.*, *27*, 1755–1758.

Zorita, E., and J. F. González-Rouco (2002), Are temperature-sensitive proxies adequate for North Atlantic Oscillation reconstructions?, *Geophys. Res. Lett.*, *29*(14), 1703, doi:10.1029/2002GL015404.

Zorita, E., J. F. González-Rouco, and S. Legutke (2003), Statistical temperature reconstruction in a 1000-year-long control climate simulation an excercise with Mann's et al. (1998) method, *J. Clim.*, *16*, 1378–1390.

H. von Storch and E. Zorita, Institute for Coastal Research, GKSS-Research Centre, Max Planck Str. 1, D-21502 Geesthacht, Germany. (zorita@gkss.de)

J. F. González-Rouco and F. Valero, Departamento de Astrofísica y CC. de la Atmósfera, Universidad Complutense de Madrid, E-28040 Madrid, Spain. (fidelgr@fis.ucm.es; valero@fis.ucm.es)

J. P. Montávez, Departamento de Física, Universidad de Murcia, E-30100 Murcia, Spain. (montavez@um.es)